Proceedings of the 11th Brazilian Congress of Thermal Sciences and Engineering -- ENCIT 2006
Braz. Soc. of Mechanical Sciences and Engineering -- ABCM, Curitiba, Brazil,- Dec. 5-8, 2006

Paper CIT06-0336

EFFECTIVE USE OF VORTEX GENERATORS TO IMPROVE THE PERFORMANCE OF SUBMERGED AIR INLETS FOR AIRCRAFT

César Celis Pérez, Luis Fernando Figueira da Silva
Department of Mechanical Engineering, Pontificia Universidade Catolica do Rio de Janeiro,
Rua Marquês de São Vicente, 225, Rio de Janeiro, RJ, 22453-900, Brazil.
{ccelis, luisfer}@mec.puc-rio.br

Sandro Barros Ferreira
Institute of Energy, Pontificia Universidade Catolica do Rio de Janeiro,
Rua Marquês de São Vicente, 225, Rio de Janeiro, RJ, 22453-900, Brazil
sandro@ituc.puc-rio.br;

Antonio Batista de Jesus, Guilherme Lara Oliveira
Empresa Brasileira de Aeronáutica SA – EMBRAER,
Avenida Brigadeiro Faria Lima, 2170, São José dos Campos, SP, 12227-901, Brazil
{antonio.jesus, guilherme.oliveira }@embraer.com.br

Abstract. *In this computational work, the influence of the use of a delta wing vortex generator upon the boundary layer that develops upstream a submerged air intake is studied. Firstly, the flow in a conventional NACA inlet is analyzed numerically and its results are considered as a reference for the comparisons with the cases in which the vortex generator is included. Then, a delta wing vortex generator is designed and assembled to the conventional NACA inlet, and the result of this assembling is studied numerically. Finally, a support mast of the vortex generator is designed, and simulations are performed of the ensemble NACA inlet with vortex generator and mast for three sideslip angles of the support. The results show that the use of the delta wing vortex generator is responsible for considerable reductions of the boundary layer thickness and, consequently, significant improvements of the performance parameters of the NACA inlet. The improvements, relative to the conventional NACA intake, in terms of ram recovery ratio and mass flow rate, are of up to 53% and 19%, respectively. The contribution of the drag induced by the vortex generator with support on the total drag of the ensemble is only about 10%.*

Keywords: *Air inlets, vortex generator, aerodynamics.*

1. Introduction

NACA inlets, Figure 1, have been widely used in aircraft as a low drag source of external flow for air conditioning, ventilation and cooling systems. The design criteria of these intakes have been established during the 1940's and 50's. Recently, classical aircraft intakes have been revisited with the use of Computational Fluid Dynamic techniques (CFD), aiming to improve their performance. Performance improvements have been sought with the use of the following techniques: (i) vortex generators (Nogueira de Faria and Oliveira, 2002 and Devine *et al.*, 2002), (ii) flow deflectors (Hall and Barclay, 1948 and Delany, 1948), (iii) parametric geometric optimization (Taskinoglu and Knight, 2004), and (iv) pulsating jets (Gorton *et al.*, 2004). None of the performance enhancement techniques explored to date has shown decisive advantage with respect to the others.

Figure 1. Conventional NACA inlet (Nogueira de Faria and Oliveira, 2002).

The boundary layer thickness upstream the air intake is the key parameter governing the performance of this type of inlets (Devine *et al.*, 2002; Hall and Barclay, 1948 and Mossman and Randall, 1948). These works show that the larger the boundary layer thickness, the poorer the performance of the air inlet. Delta wings are usually employed in supersonic airplanes, because they induce low wave drag while yielding high values of lift coefficient. These high values of lift coefficient are associated to the high levels of vorticity produced by the vortices generated along the suction side of the delta wing. In this work, the vortices generated by a delta wing vortex generator will be used to

reduce the boundary layer thickness through the mixing of high momentum air from the freestream flow with the low energy boundary layer air. The goal of this work is to evaluate the influence of the use of the delta wing vortex generator without and with support on the development of the boundary layer upstream the inlet, and, more specifically, on the performance parameters of the NACA intake. The performance parameters considered are the ram recovery ratio, the mass flow ratio or mass flow rate, and the drag coefficient. The ram recovery ratio of the NACA inlet is defined as the ratio between the dynamic pressure at the throat of the air inlet and the freestream dynamic pressure, whereas the mass flow ratio is the ratio of the actual mass flow ingested by the inlet to the mass flow that would enter to the intake at freestream conditions. The drag coefficient is computed as the ratio between the total drag, which is the component force at the direction of the freestream flow, and the freestream dynamic pressure multiplied by the throat area of the air inlet. A review of the state-of-the-art of submerged inlets, and the results of the influence of parametric variations of the vortex generator geometry were presented in previous publications (Hime *et al.*, 2005 and Celis *et al.*, 2006). This work extends the previous studies by discussing the results obtained from numerical simulations of the ensemble NACA inlet with vortex generator and support. Also, a mesh sensibility study is presented. A support mast of the vortex generator is designed, and then simulations are performed of the ensemble for three sideslip angles of the support.

2. Modeling aproach

2.1. Description of the geometric configurations

In this numerical study are simulated and analyzed three generic configurations. The conventional NACA intake, which geometric characteristics are shown in Figure 2(a), is the first configuration studied in this work. This configuration corresponds to a typical one used in a regional transport aircraft. The flow conditions analyzed correspond to a Mach number of 0.31, an altitude of 9,000 ft and a temperature of -2.83 °C. The results of this configuration will be used as a reference to evaluate the performance of the NACA intake when the vortex generator, without and with support, is utilized.

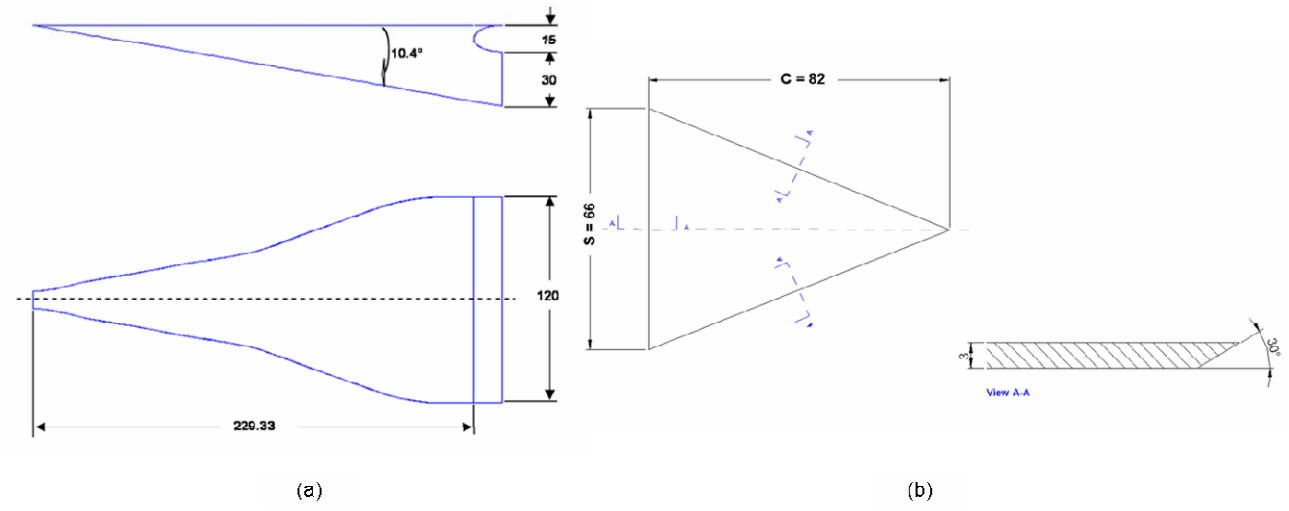

Figure 2. (a) NACA air inlet geometry, (b) Vortex generator geometry (dimensions in mm).

This conventional NACA intake is placed at the center of a flat plate of 10,000x2,000 mm^2. The inlet is positioned at a distance of 5,000 mm of the beginning of the flat plate. Aiming to simulate actual flow conditions, a duct of rectangular cross section 120x30 mm^2 and 500 mm length is coupled to the NACA inlet throat. Since the assembly NACA inlet, flat plate, and exit duct is symmetrical with respect to the center line of the NACA inlet, the configuration studied only considers half of the model. Thus, the computational domain used in the simulations consists of a parallelepiped of 10,000x1,000x1,000 mm^3, where freestream conditions are established.

The configuration resulting from the assembly of the conventional NACA inlet to the vortex generator type delta wing without support, and that in which the support mast is utilized constitute the other two generic configurations studied in this work. The main geometric characteristics of the delta wing vortex generator utilized are shown in Figure 2(b). The positioning of the vortex generator with respect to the NACA intake was defined using results from simulations of the isolated vortex generator, which will not be shown here.

2.2. Mesh generation

Grid generation of the studied configurations was performed using the commercial software ANSYS ICEM CFD, Version 5.0. All the meshes used in this work were structured meshes composed by hexahedral elements. The mesh of

the conventional NACA intake, whose shell characteristics are shown in Figure 3, was composed of about 255,000 elements.

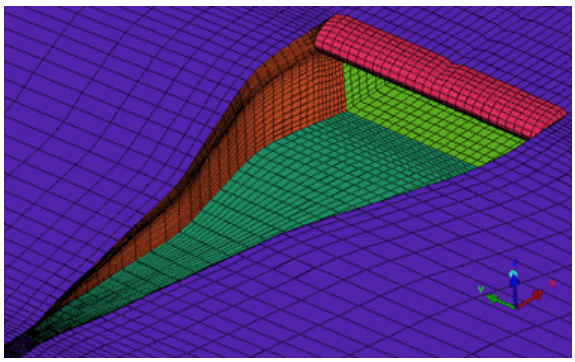

Figure 3. Shell mesh of the conventional NACA inlet.

An a priori evaluation of the quality of the elements was performed using as mesh quality parameters (i) the aspect ratio, and (ii) the angle of the elements. For hexahedral elements, the aspect ratio is defined as the ratio of the distances between diagonally opposite vertices, longer diagonal/shorter diagonal. Thus, an aspect ratio of 1 corresponds to a perfectly regular element, and an aspect ratio of infinity indicates that the element has zero volume. The angle quality parameter measures the maximum internal angle deviation from 90° for each cell. If the cells are distorted and the internal angles are small, the accuracy of the solution could be affected.

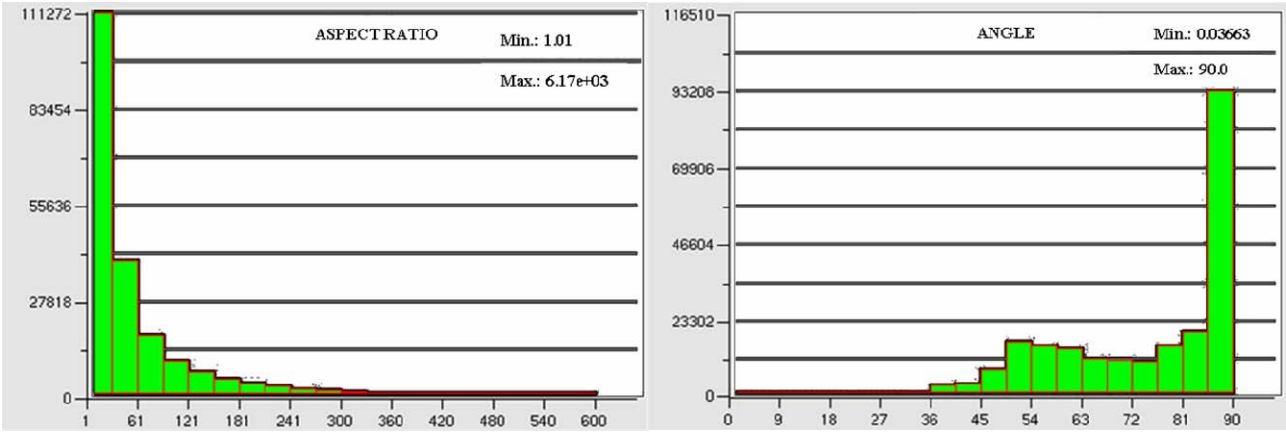

Figure 4. Mesh quality of the conventional NACA inlet.

Figure 4, which shows the histogram of distribution of the number of elements as a function of the quality parameters aspect ratio and angle, illustrates the quality of the mesh of the conventional NACA intake according to these two quality parameters. In this figure it is possible to note that the most of the elements of this mesh have an acceptable quality, aspect ratio near 1 and internal angle near 90°. However, it is clear that there are some elements (< 1%) with a quality smaller than could be desirable. These elements are located on regions of the flow where the mesh is very refined. In the results section it will be shown that the quality of this small group of elements does not affect the solution.

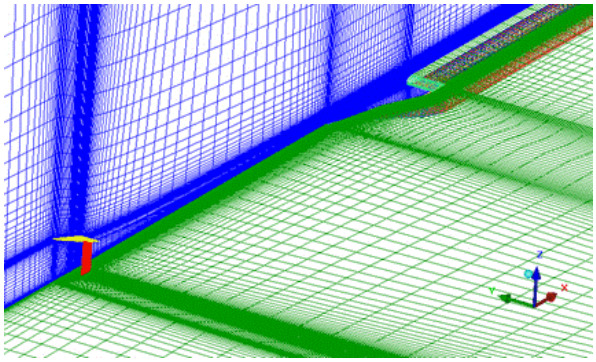

Figure 5. Computational mesh, NACA inlet with vortex generator and support.

The computational mesh used to simulate the flow on the configurations of NACA inlet with vortex generator without support consisted of nearly 1,100,000 elements. The details of the meshes used to simulate the flow on these configurations will not be shown because their similarity with those used at the configurations of NACA intake with vortex generator and support. The meshes used at these configurations of NACA intake with vortex generator and support, one of which is shown in Figure 5, consisted of approximately 1,700,000 elements. On all the configurations corresponding to the NACA inlet with vortex generator without and with support an analysis of mesh quality, similar to that performed on the conventional NACA inlet, was performed in order to verify the quality of the meshes utilized, and thus to ensure an appropriate description of the flow around the NACA inlet and the vortex generator.

2.3. Flow solver

All the numerical simulations were conducted using the commercial CFD package FLUENT, Version 6.1. For the resolution of the governing equations of the compressible flow, Fluent uses a control-volume-based technique, which consists of the division of the domain into discrete control volumes using a computational grid. The integration of the governing equations on the individual control volumes allows constructing algebraic equations for the discrete dependent variables. The linearization of the discretized equations and solution of the resultant linear equation system yields updated values of the dependent variables.

In this work, an implicit segregated solver was used to solve the governing equations along with a Spalart-Allmaras (Spalart and Allmaras, 1994) turbulence model. The interpolation scheme used for the convection term was the Second-Order Upwind Scheme, and the Second-Order for calculating face Pressure. The algorithm applied for Pressure-Velocity Coupling was SIMPLE (Semi-Implicit Method for Pressure-Linked Equations).

2.4. Boundary and initial conditions

Figure 6 illustrates the computational domain zones where the boundary conditions were set. At the farfield, zone 1 (dashed blue lines), freestream conditions with a given Mach number, static pressure and temperature were specified. At the duct exit section, zone 2 (green line), a constant static pressure was specified. No-slip adiabatic boundary conditions were set at the solid walls, zone 3 (red lines). Finally, symmetry conditions were set at the symmetry plane of both the conventional NACA intake and the vortex generator.

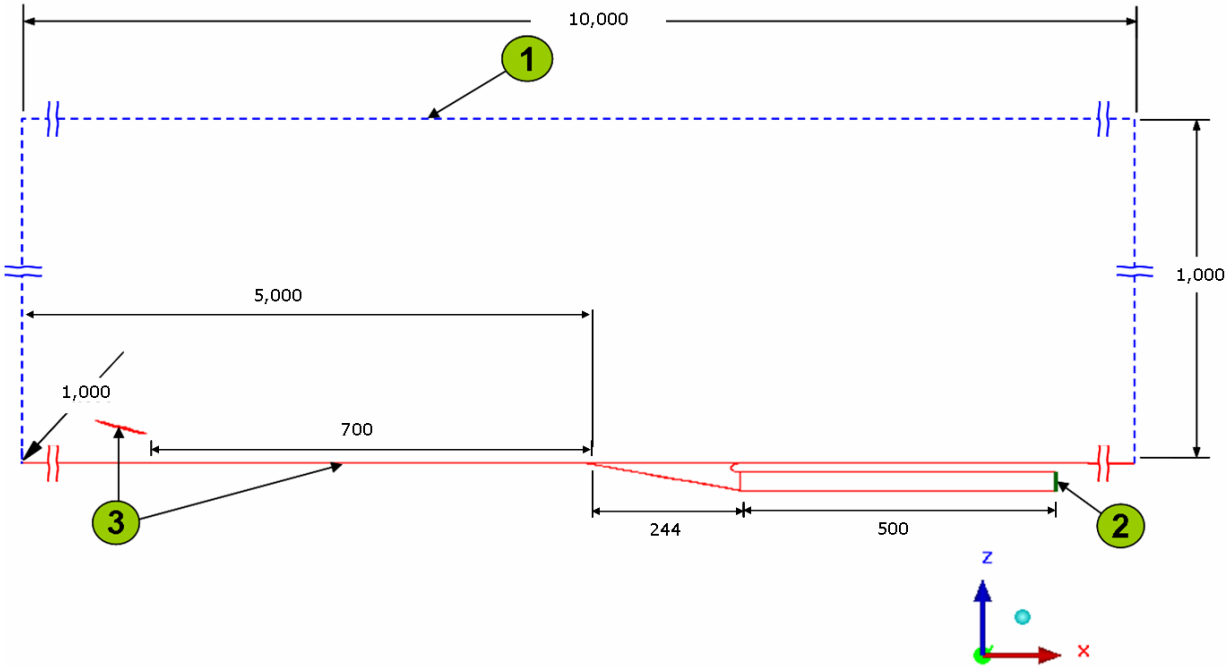

Figure 6. NACA inlet with vortex generator and support – Symmetry plane (dimensions in mm).

The computations were initialized from freestream flow conditions given in Table 1.

Table 1. Freestream flow conditions.

Pressure (p)	Pa	72,428
Temperature (T)	K	270.3
Mach number (M)	-----	0.31
Modified Turbulent Viscosity	m^2/s	0.001

3. Results and discussion

Table 2 summarizes the configurations studied in this work. In this table, β represents the sideslip angle of the support of the vortex generator. In all the configurations of NACA intake with vortex generator showed in this work, the horizontal distance between the trailing edge of the vortex generator and the beginning of the ramp of the NACA inlet was 700 mm, the angle of attack (α) of the vortex generator was 15°, and the vertical distance between the trailing edge of the vortex generator and the flat plate was 50 mm. The area of the vortex generator was A = 2,706 mm^2. For the sake of simplicity, the results will be referenced to their respective codes indicated in Table 2.

Regarding the convergence criterion of the simulated cases in this work, it is important to emphasize that, in all the computations performed here, the solver execution was interrupted only after the residuals of all the computed variables achieved their complete stabilization. The residual levels of all the variables after the stabilization were of the order of 10^{-4} or lesser, except in the case of the mass conservation in which the residuals were of the order of 10^{-2}. The approximated iterations number necessary to achieve the complete stabilization of the residual was of 6,000, 10,000, and 25,000, for the configurations corresponding to the conventional NACA inlet, the NACA inlet with vortex generator, and the NACA inlet with vortex generator and support, respectively.

Table 2. Summary of the configurations simulated.

Case	β (°)
N1A-1	DATUM
NGVA	VG without support
NGVAM-0	0
NGVAM-5	5
NGVAM-10	10

3.1. Conventional NACA inlet

3.1.1. Flow structure

It is well known that the boundary layer thickness is a determinant parameter of the efficiency of a NACA inlet. So, in order to characterize the influence of the vortex generator upon the boundary layer, plots representing the boundary layer development upstream the NACA inlet will be analyzed throughout the paper. Moreover, since conventional NACA inlets have their design based on the generation of vorticity on the divergent ramp walls, contours illustrating the level of vorticity will be also shown. Figure 7 shows cross sections, in transversal planes to the external flow direction, of the longitudinal velocity contours for the configuration of the conventional NACA inlet, case N1A-1. This figure allows verifying the thick boundary which develops upstream the NACA inlet. From computations it was determined that the boundary layer thickness at the beginning of the ramp of the NACA intake is about 50 mm. Also, it is clear that the inlet ingests mostly low energy fluid.

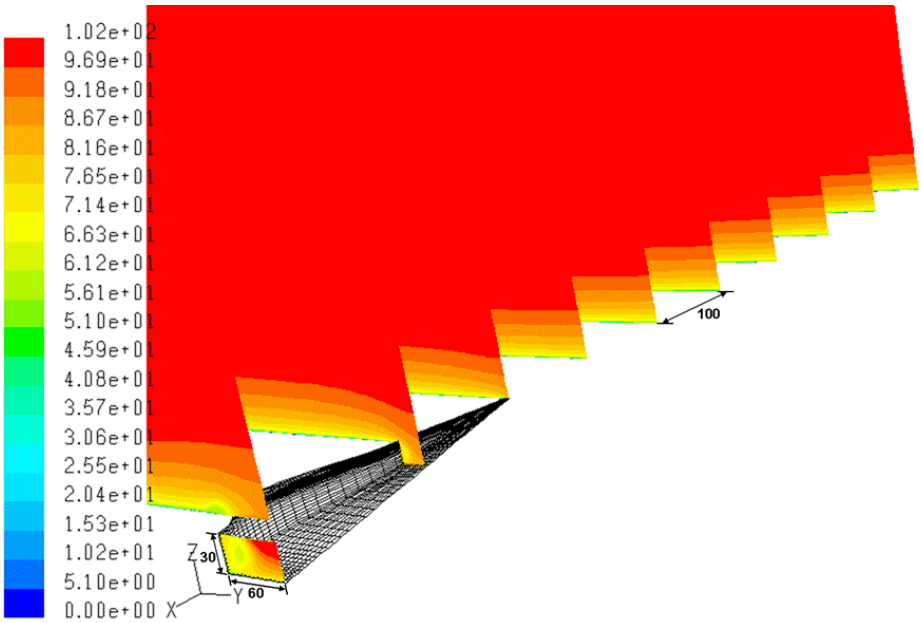

Figure 7. Longitudinal velocity (m/s) – Case N1A-1 (dimensions in mm).

Figure 8 shows the evolution of the longitudinal component of the vorticity for the case of the conventional NACA inlet, case N1A-1, in the same transversal planes to the external flow direction. In this figure, it is possible to see, clearly, the high levels of vorticity originated at the regions close to ramp walls of the NACA inlet. Note that the operation of this type of inlet is based on the generation of vortices on the ramp walls as a consequence of its particular geometry. Consequently, the flow on the throat of NACA inlet is tridimensional.

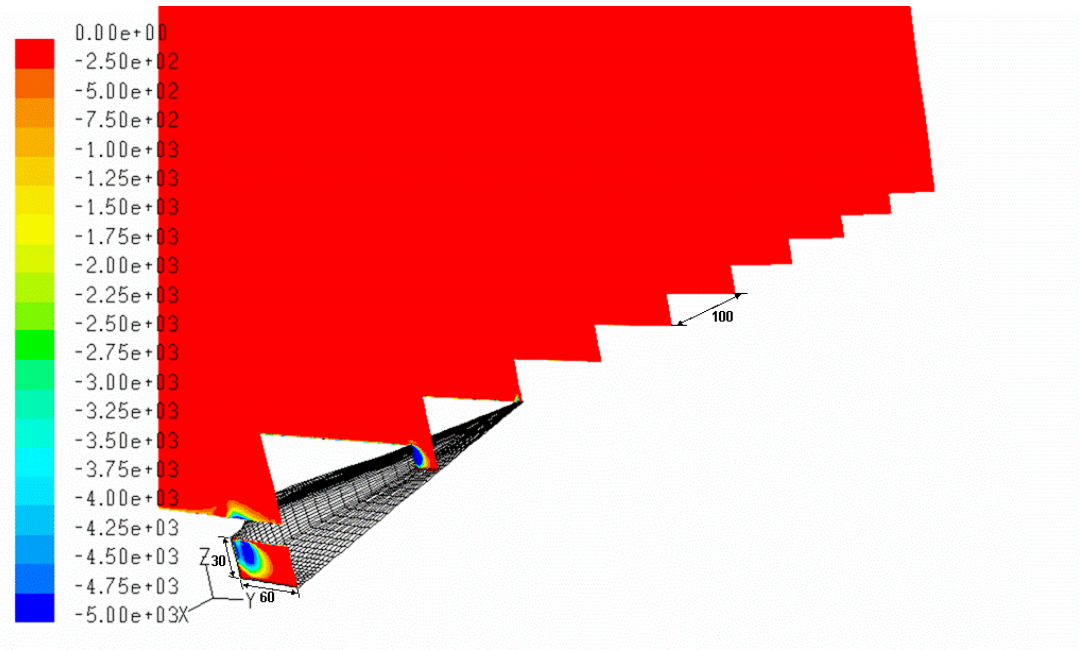

Figure 8. Longitudinal vorticity (1/s) – Case N1A-1 (dimensions in mm).

3.1.2. Influence of the level of refinement of the computational mesh

In order to analyze the influence of the level of refinement of the computational mesh used in the numerical simulations of the conventional NACA inlet on the values of its performance parameters, the mesh utilized was refined using one of the methods of solution-adaptive refinement available in Fluent. The adaptive refinement process utilized is based on the use of a gradient adaption function, which is defined as a function of the element volume and the Euclidean norm of the gradient of the selected solution variable. Trough the use of this gradient adaption function it is assumed that maximum error occurs in high-gradient regions. This particular adaptive refinement process requires (i) the choice of the solution variable from which the adaption function will be constructed, and (ii) for this solution variable, the refine threshold from which the mesh will be refined by subdivision of its elements. Two adaptive refinement processes were performed in this work. The first refinement process was performed using, as solution variable, the longitudinal component of the velocity. In this case, the refine threshold was specified as equal to 5, i.e., elements with gradient values above this value were refined. In the second refinement process the static pressure was considered as solution variable. In this second case, the refine threshold was specified as equal to 10. Modifications of these refinement thresholds in order to assess their influence of the obtained results were not performed.

The number of elements on the mesh after the adaptive refinement process based on the velocity gradients was about 998,000 and about 770,000 after the refinement process based on the static pressure gradients, whereas the original mesh contained about 255,000 elements. From analyses of the meshes obtained after the refinement processes, it was verified that the refinement processes increased the number of elements of the mesh at the regions where the longitudinal component of the velocity and the static pressure present the greatest gradients, i.e., exit duct, ramp, and lip angle of the NACA inlet.

Regarding the performance parameters of the conventional NACA inlet, Table 3 shows the values of these parameters, which were computed using the results obtained from the numerical simulations, for the configuration of the conventional NACA intake, N1A-1, and for the cases in which the adaptive refinement processes was utilized. This table also shows the data used to design this particular NACA inlet. It is important to highlight that the values of ram drag, shown in this table, were computed from equations 3.18 and 6.1 of the ESDU 86002 (Engineering Sciences Data Unit, ESDU, 1996). The friction drag was calculated as the integral wall shear stress of the NACA inlet. Neither the flat plate nor the duct was considered for this drag calculation. The mass flow rate was obtained by a direct integration at the duct exit section of the NACA intake.

Table 3 allows verifying that a good agreement was obtained between the computed values of the performance parameters and the design data. Note, also, that the value of the computed friction drag is negligible when compared to the value of the ram drag of the NACA inlet. Even though the adaptive mesh refinement process more than doubles the

number of elements, the resulting values of the performance parameters of the NACA inlet do not show significant discrepancies, such as can be seen in Table 3. The results reported in this table show that the original mesh used to simulate the NACA inlet, i.e., the mesh without refinement, is already satisfactory to describe the flow behavior through the NACA inlet. When the mesh adaption process was performed, variations of only 1%, in terms of ram recovery ratio, drag coefficient and mass flow rate, were found. Therefore, the level of refinement used on the baseline mesh is considered satisfactory and will be applied to the different meshes used in the computations where the vortex generator is included.

Table 3. Performance parameters – Conventional NACA inlet without and with adaptive refinement.

Parameters	Design Data	N1A-1	Refinement: X velocity	Refinement: S. pressure
Ram-recovery ratio	0.550	0.513	0.511	0.519
Mass-flow rate [kg/s]	0.260	0.260	0.259	0.261
Mass-flow ratio, MFR	----	0.76	0.76	0.76
Total drag, Td = Rd+Fd [N]	16.41	18.60	18.45	18.59
Ram drag, Rd = a+b+c [N]	----	18.13	17.97	18.11
(a) NACA	----	18.13	17.97	18.11
(b) VG	----	0.00	0.00	0.00
(c) Support	----	0.00	0.00	0.00
Friction drag, Fd = d+e+f [N]	----	0.47	0.48	0.47
(d) NACA	----	0.47	0.48	0.47
(e) VG	----	0.00	0.00	0.00
(f) Support	----	0.00	0.00	0.00
Drag coefficient	0.93	1.06	1.06	1.06

3.1.3. Validation of the numerical results

It is important to emphasize that literature on submerged intakes is practically inexistent between the mid 1950s and the end of the 1990s. Apparently, during this period no works were developed related to the submerged inlets. The work performed on the 1940s and 1950s is, as it could be expected, focused on experiments. The main goal of these works, which were conducted by the National Advisory Committee for Aeronautics (NACA), was to determine the influence of both the flow parameters and the geometric configuration on the performance parameters of this type of intakes. Within the references reviewed (Hime *et al.*, 2005), few had detailed information about the flow field, what makes the comparison between the results described and a Computational Fluid Dynamics (CFD) simulation impossible. In particular, among the references reviewed, velocity measurements were not available. Roughly speaking only total pressure is measured. Such an experimental flowfield characterization is insufficient for the purpose of choosing the most appropriate turbulence model. Then, since detailed experimental results are not available to validate the numerical results obtained in this work, design data obtained from ESDU will be used as a reference to validate these computational results and to select the more appropriate turbulence model to simulate the flow in the NACA intake. Thus, Figure 9 shows curves of ram recovery ratio, for the results obtained from the ESDU 86002, and from numerical simulations performed using as turbulence model both the Spalart-Allmaras and the k-ε Realizable (Shih *et al.*, 1995) turbulence model.

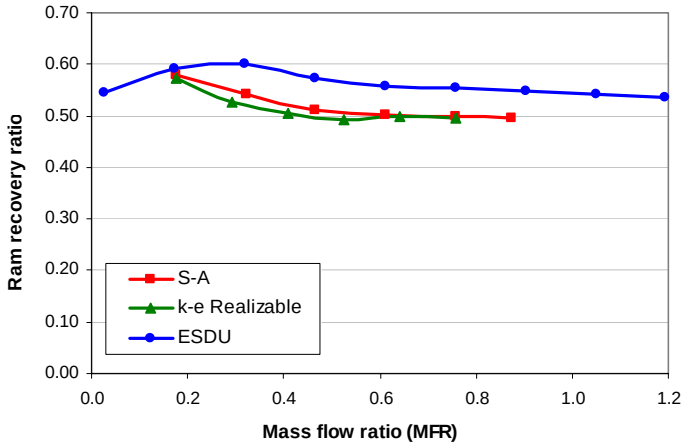

Figure 9. Ram recovery ratio of the conventional NACA intake as a function of the mass flow ratio.

In Figure 9 it is possible to verify that the numerical simulations under-estimate the values of the ram recovery ratio of the NACA inlet. Furthermore, the value of the mass flow ratio of maximum ram recovery ratio is under predicted by the computations. However, in this figure one can observe that the performance trends computed with both turbulence models are quite similar to each other, even if the semi-empirical figures computed from ESDU always exhibit higher values. Considering that the computed values of ram recovery ratio using the Spalart-Allmaras turbulence model showed the smallest discrepancies, about 8%, when compared to the design data obtained from ESDU, and that this turbulence model was specifically developed for aerodynamical applications, it was decided to use only this model on the simulations performed in this work.

3.2. NACA inlet with vortex generator

The influence of the use of the delta wing vortex generator upon the development of the boundary layer upstream the NACA inlet and, consequently, on the performance parameters of this type of intakes, is analyzed using the same plots used to describe the flow structure in the case of the conventional NACA intake.

Figure 10 shows cross sections, in transversal planes to the external flow direction, of the longitudinal velocity contours for the basic configuration of NACA inlet with vortex generator, called NGVA. In this figure, considering that the free-stream velocity at x-axis direction is equal to 102 m/s, it is possible to see, accordingly to the color scale, that the downwash effect of the vortices generated by the delta wing vortex generator leads to a considerable reduction of the boundary layer thickness upstream the air intake, which occurs mainly at the central region of the flat plate. One immediate consequence of the reduction of the boundary layer thickness is the larger amount of external air ingested by the NACA intake, which leads to increases of the ram recovery ratio and the mass flow rate, such as will be demonstrated later.

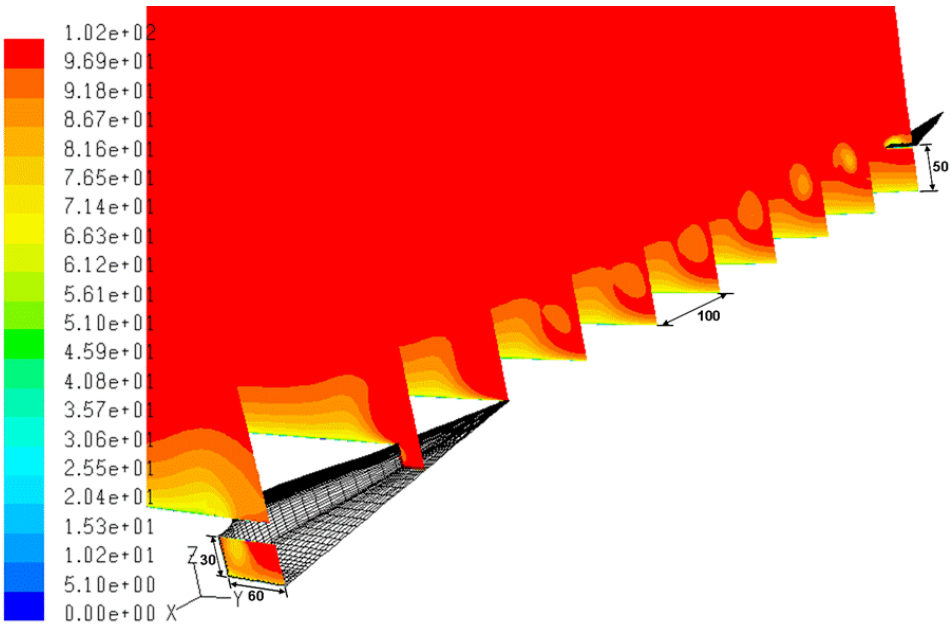

Figure 10. Longitudinal velocity (m/s) – Case NGVA (dimensions in mm).

The considerable reduction of the boundary layer thickness upstream the air intake observed in Figure 10 is originated, as mentioned previously, by the downwash effect of the vortices generated at the suction side of the vortex generator, which are shown in Figure 11. This figure shows the evolution of the longitudinal component of the vorticity for the case of the basic configuration of NACA inlet with vortex generator, case NGVA, in the same transversal planes to the external flow direction. Figure 11, which clearly shows the development of these vortices and the high levels of vorticity associated with them, allows observing that the vortex cores are not ingested by the intake. This particular behavior avoids the negative effects that the vortices ingestion could originate. Comparing this figure with Figure 8, case N1A-1, it is possible to see that the presence of the vortex generator originates, at the throat plane of the NACA inlet, a greater region affected by the vorticity. However, these higher levels of vorticity are not detrimental to the inlet performance, as shown further on.

3.3. NACA inlet with vortex generator and support

The next stage on the development of our work was to design the support of the vortex generator which is used to maintain the desired relative position with respect to the NACA intake. To this end, it was considered that the support should, if possible, contribute to the reduction of boundary layer thickness upstream the NACA intake and downstream

the vortex generator. Considering this aspect, what one intends is that the wake generated by the support can contribute positively to the effect of the counter-rotating vortices generated on the suction side of the vortex generator, and specifically, to supplement the effect of these vortices on the reduction of the boundary layer thickness. Since the reduction of the boundary layer thickness occurs mainly on the central region of the flat plate, it was decided to use a pair of tip-mounted supports. Another possibility considered was the use of a ventral support, which was cast aside since the wake generated by this type of support could (i) negatively influence the process of reduction of the boundary layer thickness, and (ii) be ingested by the NACA intake, degrading its performance parameters.

The basic configuration of NACA intake with vortex generator, called NGVA, was used as the configuration on which the support was designed. The designed support was obtained as a result of the extrusion, at the normal direction to the flat plate, of a NACA 0012 profile, whose chord is 25 mm. The distance, in the lateral direction, between the leading edge of the support and the symmetry plane of the vortex generator is 21 mm. Defining the angle formed by the chord of the support and the symmetry plane of the vortex generator as "sideslip angle", β, it was decided to perform computations for different values of the sideslip angle, in order to evaluate its influence on the performance parameters of the NACA inlet. Note that it is expected that the actual flow sideslip angle should be different from the geometrical sideslip, since the pressure difference between the suctions and the pressure side of the vortex generator induces lateral flow.

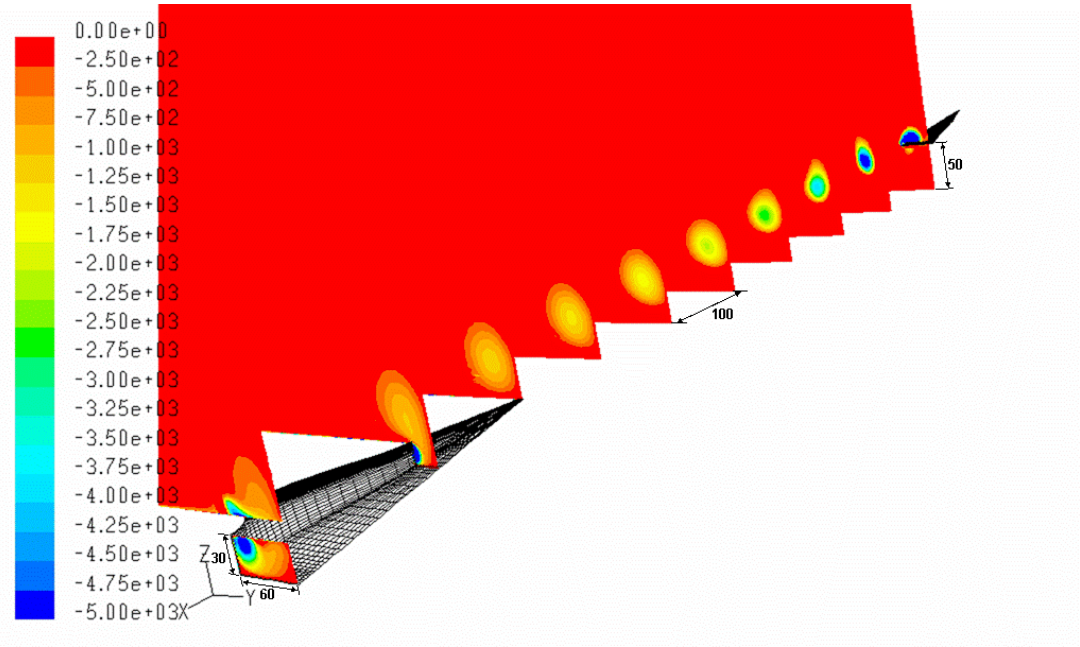

Figure 11. Longitudinal vorticity (1/s) – Case NGVA (dimensions in mm).

3.3.1. Flow structure

Figure 12 shows cross sections, in transversal planes to the external flow direction, of the longitudinal velocity contours for the basic configuration of NACA inlet with vortex generator and support, NGVAM-0. Comparing this figure with Figure 10, corresponding to the basic configuration of NACA inlet with the freely standing vortex generator, it is possible to see that that the boundary layer development upstream the NACA inlet and downstream the vortex generator is slightly influenced by the presence of the support of the vortex generator. This influence seems to be restricted to the first 200 mm downstream the vortex generator, where occurs a reduction of the velocity due to the wake generated by the support. Further downstream the vortex generator, the boundary layer thickness does not present significant variations originated by the presence of the support. Thus, the use of the vortex generator and its support continues to lead to a considerable reduction of the boundary layer thickness upstream the air intake, and, consequently, significant improvements of the performance parameters of the NACA intakes are obtained, such as will be shown further on.

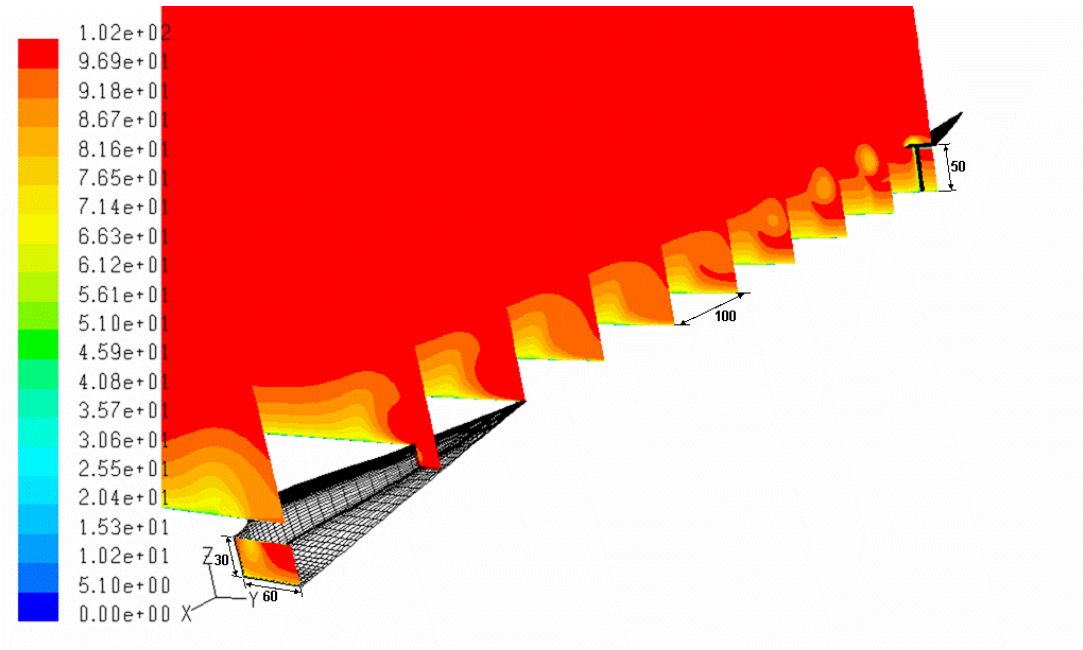

Figure 12. Longitudinal velocity (m/s) – Case NGVAM-0 (dimensions in mm).

The longitudinal vorticity contours for the basic configuration of NACA inlet with vortex generator and support, NGVAM-0, which allows observing the behavior of the vortices wake generated by the support, is shown in Figure 13. This figure clearly shows that the intensity of the vorticity at the wake generated by the support is small when compared to the vortices generated on the suction side of the vortex generator. In this figure, also it is possible to see that support wake is displaced away from the symmetry plane due to the effect of the vortex generator wake and completely dissipated upstream the beginning of the ramp of the NACA inlet.

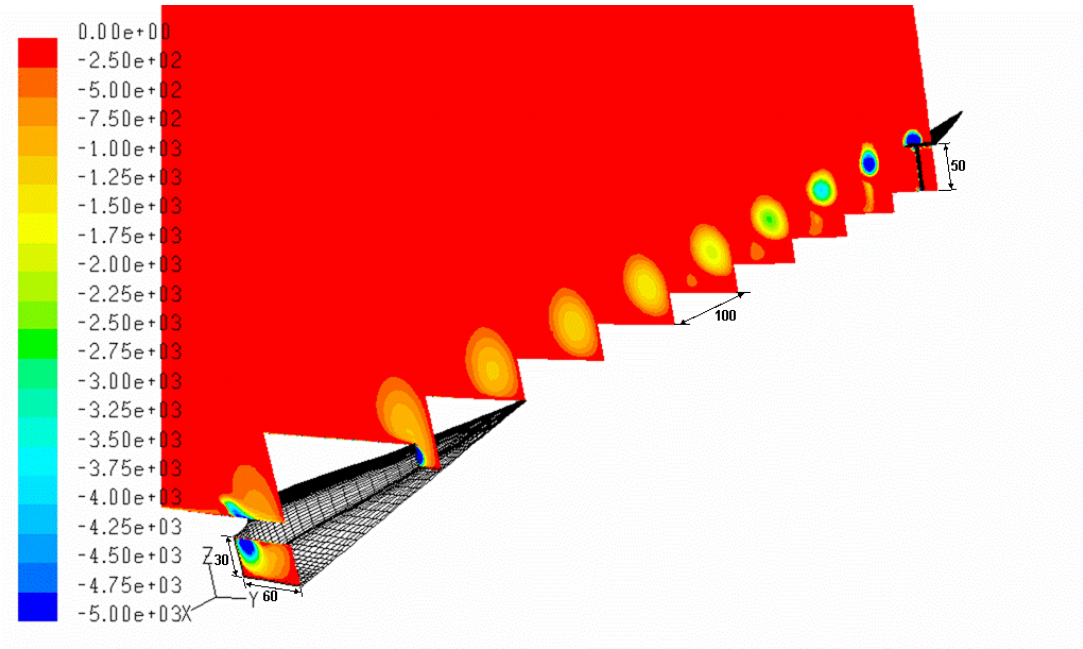

Figure 13. Longitudinal vorticity (1/s) – Case NGVAM-0 (dimensions in mm).

3.3.2. Influence of the sideslip angle of the support of the vortex generator

With the aim of assessing the influence of the sideslip angle of the vortex generator support on the performance parameters of the NACA intake, two different values of the sideslip angle of the support, 5° and 10°, configurations NGVAM-5 and NGVAM-10, respectively, were studied. Figure 14 and Figure 15 show cross sections, in transversal planes to the external flow direction, of the longitudinal velocity contours for the configurations NGVAM-5 and NGVAM-10, respectively. In these figures it is possible to verify that for the two values of the sideslip angle of the support, i.e., β = 5° and 10°, the reduction of the boundary layer thickness at the central region of the flat plate remains

practically unaltered. These figures also show that the wake of the support seems to enhance the lateral motion of the fluid downstream the vortex generator.

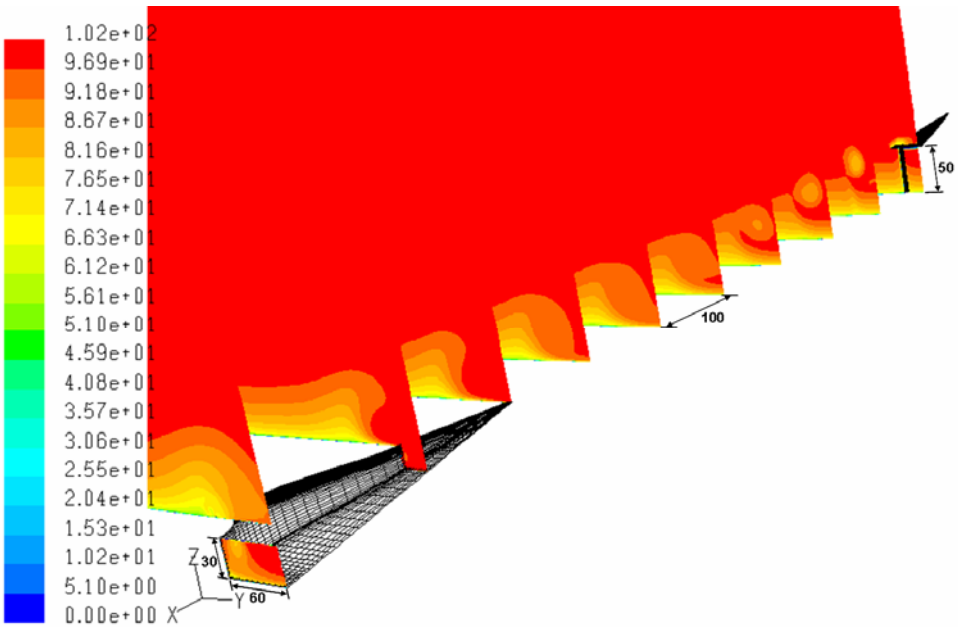

Figure 14. Longitudinal velocity (m/s) – Case NGVAM-5 (dimensions in mm).

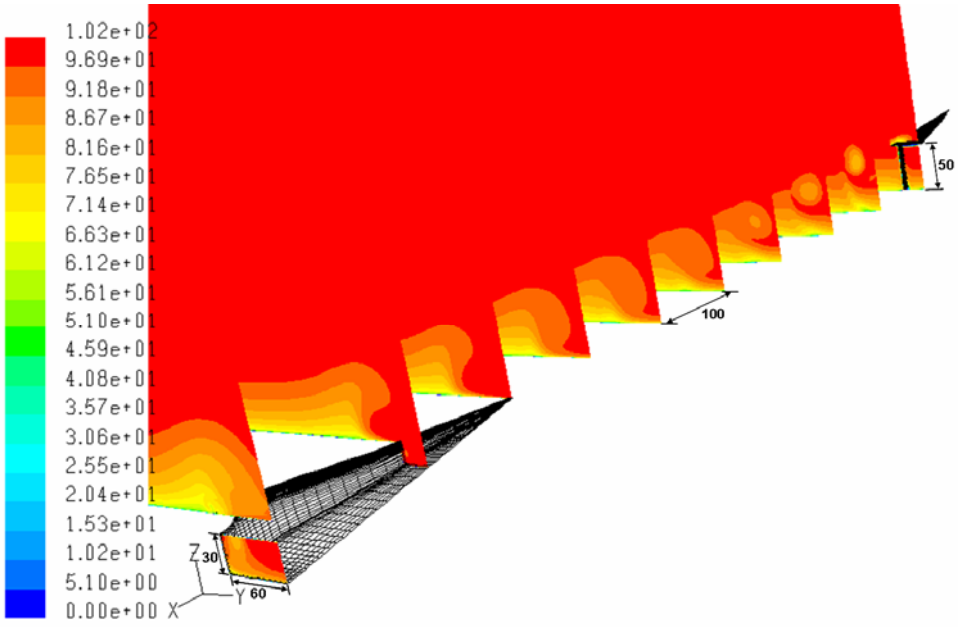

Figure 15. Longitudinal velocity (m/s) – Case NGVAM-10 (dimensions in mm).

Figure 16 and Figure 17 show the longitudinal vorticity contours, in the same transversal planes to the external flow direction, for the configurations of NACA inlet with vortex generator and support which are being analyzed, i.e., NGVAM-5 and NGVAM-10. In these figures it is possible to verify that the longitudinal component of the vorticity practically disappears with the increase of the sideslip angle of the support to 10°. This result is in accordance with design specifications of the support, which intended to minimize the negative effects of the presence of the support on the performance parameters of the NACA intake. Indeed, at the sideslip angle of 10°, the mast profile is aligned with the local flow deflection angle at the suction side of the vortex generator, thus leading to a lesser interference.

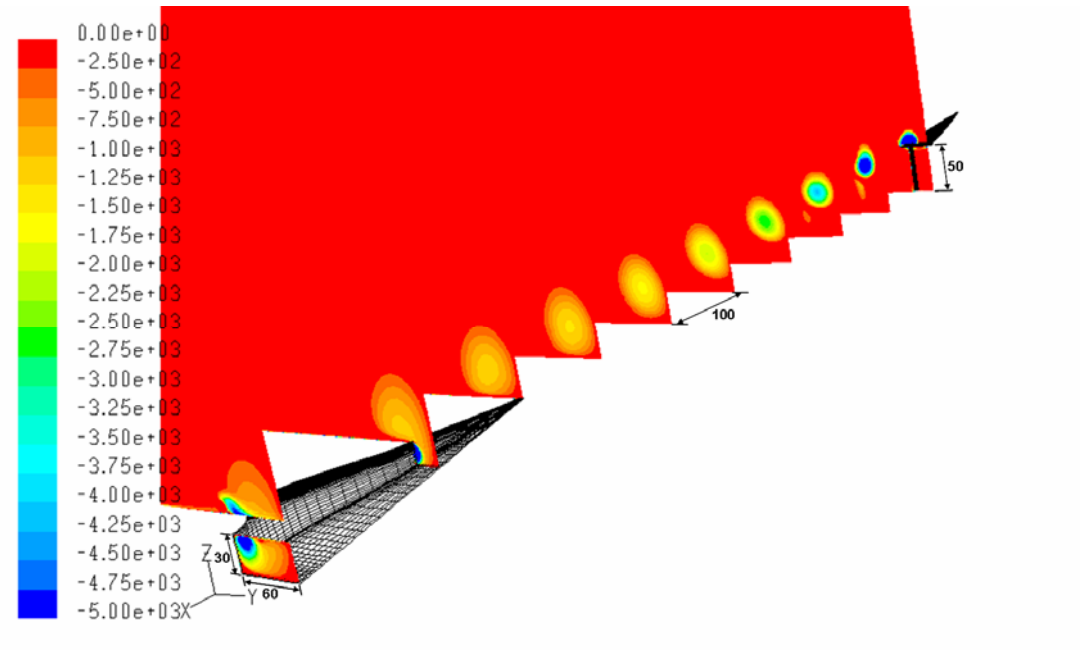

Figure 16. Longitudinal vorticity (1/s) – Case NGVAM-5 (dimensions in mm).

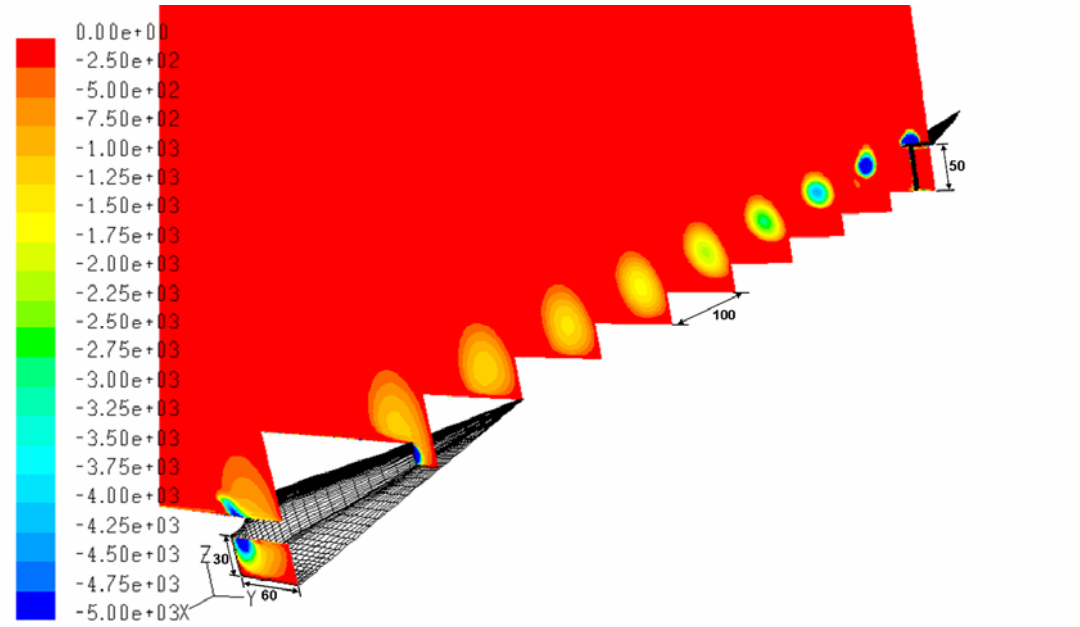

Figure 17. Longitudinal vorticity (1/s) – Case NGVAM-10 (dimensions in mm).

Table 4 shows the values of the performance parameters for the conventional NACA intake, for the basic configuration of NACA inlet with vortex generator without and with support, and for the two configurations of NACA inlet with vortex generator and support called NGVAM-5 and NGVAM-10, which are being analyzed. These parameters were computed following the same procedures used for the conventional NACA inlet, but now accounting for the contribution of the vortex generator and its support to both the ram drag and the friction drag. In this table, the percentage increases related to the values of the performance parameters corresponding to the conventional NACA inlet are indicated in the parentheses.

The results shown in Table 4 indicate that the considerable reduction of the boundary layer thickness upstream the air intake, observed in Figure 10, Figure 12, Figure 14 and Figure 15, leads to significant improvements of the ram recovery ratio and the mass flow rate. This is a direct consequence of the larger amount of external air ingested by the NACA intake. Table 4 also indicates that the presence of the support does not negatively affect the values of the performance parameters of the NACA intake. On the contrary, it contributes to slightly increase the overall performance of the intake. Thus, this table shows that the three configurations of the NACA inlet with vortex generator and support

exhibit improvements for the computed values of mass flow rate and ram recovery ratio. The largest increases in these performance parameters are obtained for a sideslip angle of the support of 10°.

Table 4. Performance parameters – Influence of the sideslip angle of support of the vortex generator.

Parameters	Design Data	N1A-1	NGVA	NGVAM-0	NGVAM-5	NGVAM-10
Ram-recovery ratio	0.550	0.513	0.741 (44.4 %)	0.749 (46 %)	0.774 (50.9 %)	0.787 (53.3 %)
Mass-flow rate [kg/s]	0.260	0.260	0.302 (16 %)	0.303 (16.5 %)	0.307 (18.1 %)	0.309 (18.9 %)
Mass-flow ratio, MFR	----	0.76	0.88 (16 %)	0.88 (16.5 %)	0.9 (18.1 %)	0.9 (18.9 %)
Total drag, Td = Rd+Fd [N]	16.41	18.60	32.43 (74.4 %)	33.18 (78.4 %)	33.67 (81 %)	34.31 (84.5 %)
Ram drag, Rd = a+b+c [N]	----	18.13	31.69 (74.7 %)	32.34 (78.3 %)	32.8 (80.9 %)	33.45 (84.4 %)
(a) NACA	----	18.13	29.68 (63.7 %)	29.81 (64.4 %)	30.22 (66.7 %)	30.43 (67.8 %)
(b) VG	----	0.00	2.01	2.35	2.21	2.09
(c) Support	----	0.00	0.00	0.18	0.37	0.93
Friction drag, Fd = d+e+f [N]	----	0.47	0.74 (60 %)	0.84 (80.1 %)	0.86 (85.8 %)	0.87 (86 %)
(d) NACA	----	0.47	0.59 (26.5 %)	0.58 (24.2 %)	0.59 (26.8 %)	0.6 (29.2 %)
(e) VG	----	0.00	0.16	0.15	0.15	0.15
(f) Support	----	0.00	0.00	0.11	0.13	0.11
Drag coefficient	0.93	1.06	1.86 (74.4 %)	1.9 (78.4 %)	1.93 (81 %)	1.96 (84.5 %)

Besides, in Table 4 it can be seen that in the three configurations of NACA inlet with vortex generator and support, the drag coefficient values only exhibit a small increase when compared to the corresponding values of the case called NGVA. The reason behind this slight increase observed is related to the fact that the contribution to the ram drag, the main component of the total drag, due to the presence of the support is negligible when compared to that of the NACA inlet. However, when the values of the drag coefficient of the configurations of NACA inlet with vortex generator without and with support are compared to that of the conventional NACA inlet, it is possible to verify that the obtained increases are considerable. This is a direct consequence of the increase of mass flow rate that follows the reduction of the boundary layer thickness. Even so, the drag contribution due to the vortex generator with support is only about 10% of the total drag of the ensemble. In this case, 7% corresponds to the drag produced by the vortex generator and 3% to the support of the vortex generator. It is worthy to highlight that the contribution of this 10% relative increase on the drag due the vortex generator with support on the total drag of the aircraft is insignificant. This type of performance enhancement device should be used only in certain NACA inlets, such as that corresponding to the Auxiliary Power Unity.

4. Conclusions and perspectives

In this computational work the influence of the use of a delta wing vortex generator upon the boundary layer that develops upstream the air intake, with the aim of decreasing its thickness and thus to improve the performance of a NACA inlet, was investigated. The values of the ram recovery ratio of the conventional NACA inlet computed from the results obtained from numerical simulations show that there is a good agreement when compared to their respective design data. Regarding the adaptive refinement process of the computational mesh utilized, the results show that the adopted refinement process does not have a significant influence on the obtained results. The differences obtained with relation to the original mesh, which are about 1%, allow concluding that, regarding the performance parameters, the obtained results present mesh convergence.

The computational results show that the presence of the freely standing vortex generator is responsible for considerable reductions of the boundary layer thickness and, consequently, significant improvements of the performance parameters of the NACA inlet. The obtained improvements, relative to the conventional NACA intake, in terms of ram recovery ratio and mass flow rate, are 44% and 16%, respectively. When the support of vortex generator was utilized, additional improvements of the performance parameters of the NACA inlet were obtained. For the this case, improvements of up to 53%, in terms of ram recovery ratio, and 19%, in terms of mass flow rate ingested by the intake, were achieved. The contribution of the drag induced by the presence of the vortex generator with support on the total drag of the ensemble is small, only about 10%. The choice of using – or not – vortex generators to increase NACA inlet performance is, obviously, a designer choice.

In order to validate the results obtained in this work, an associated experimental study is needed, in which detailed measurements would allow validating the numerical results obtained. Also, future work should involve the study of other parametric variations, including combinations of those already studied, in order to optimize the vortex generator geometry.

5. Acknowledgements

The authors wish to thank Embraer, CNPq and Fapesp for the support provided for this work. During this work Luís Fernando Figueira da Silva was on leave from the Laboratoire de Combustion et de Détonique (Centre National de la Recherche Scientifique, France). Mesh generation was performed by Mr. Rodrigo Ferraz, from ESSS (Engineering Simulation and Scientific Software Ltda).

6. References

Celis, C. P., Figueira da Silva, L. F., Ferreira, S. B., Batista de Jesus, A., and Oliveira, G. L., "Numerical Study of the Performance Improvement of Submerged Air Intakes using Vortex Generators", 25th ICAS Congress, Hamburg, Germany, Sept. 2006.

Delany, N. K., "An Investigation of Submerged Air Inlets on a ¼-scale Model of a Fighter-type Airplane", NACA RM A8A20, June 1948.

Devine, R. J., Watterson, J. K., Cooper, R. K., and Richardson, J., "An Investigation into Improving the Performance of Low Speed Auxiliary Air Inlets using Vortex Generators", 20th AIAA Applied Aerodynamics Conference, AIAA 2002-3264, St. Louis - Missouri, June 2002.

Engineering Sciences Data Unit, ESDU, "Drag and Pressure Recovery Characteristics of Auxiliary Air Inlets at Subsonic Speeds", Item Nº 86002 with amendments A and B, London 1996.

Gorton, S. A., Owens, L. R., Jenkins, L. N., Allan, B. G., and Schuster, E. P., "Active Flow Control on a Boundary-Layer Ingesting Inlet", 42nd AIAA Aerospace Sciences Meeting and Exhibit, AIAA 2004-1203, Reno - NV, Jan. 2004.

Hall, C. F., and Barclay, F. D., "An Experimental Investigation of NACA Submerged Inlets at High Subsonic Speeds. I-Inlets Forward of the Wing Leading Edge", NACA RM A8B16, June 1948.

Hime, L., Celis, C. P., Figueira da Silva, L. F., Ferreira, S. B., Batista de Jesus, A., Takase, V. L., and Vinagre, H. T. M., "A Review of the Characteristics of Submerged Air Intakes", 18th International Congress of Mechanical Engineering, COBEM2005-1016, Ouro Preto - MG - Brazil, Nov. 2005.

Mossman, E. A., and Randall, L. M., "An Experimental Investigation of the Design Variables for NACA Submerged Duct Entrances", NACA RM A7130, Jan. 1948.

Nogueira de Faria, W., and Oliveira G. L., "Análise de Entradas de Ar tipo NACA com Gerador de Vórtices", 9th Brazilian Congress of Thermal Engineering and Sciences - ENCIT 2002, CIT02-0758, Caxambu - MG - Brazil, Nov. 2002.

Shih, T. H., Liou, W. W., Shabbir, A. and Zhu, J., "A New k-Eddy-Viscosity Model for High Reynolds Number Turbulent Flows - Model Development and Validation", Computers and Fluids, Vol. 24, No. 3, 1995, pp. 227-238.

Spalart, P. R., and Allmaras, S. R., "A One-Equation Turbulence Model for Aerodynamic Flows", La Recherche Aérospatiale, No. 1, 1994, pp. 5-21.

Taskinoglu, E. S., and Knight, D. D., "Multi-Objective Shape Optimization Study for a Subsonic Submerged Inlet", Journal of Propulsion and Power, Vol. 20, No. 4, 2004, pp.620-633.